The use of Singular Functions

for the

Approximate Conformal Mapping

of

Doubly-Connected Domains

by

N. Papamichael and C.A. Kokkinos*

* On study leave from the National Technical University of Athens.

(per)
QA
1
B78

w9260139

ABSTRACT

Let f be the function which maps conformally a given doubly-connected domain onto a circular annulus. We consider the use of two closely related methods for determining approximations to f of the form

$$f_n(z) = z \exp\left\{ \sum_{j-1}^{n} a_j u_j(z) \right\},$$

where $\{u_j\}$ is a set of basis functions. The two methods are respectively a variational method, based on an extremum property of the function

$$H(z) = f'(z)/f(z) - 1/z,$$

and an orthononnalization method, based on approximating the function H by a finite Fourier series sum.

The main purpose of the paper is to consider the use of the two methods for the mapping of domains having sharp corners, where corner singularities occur. We show, by means of numerical examples, that both methods are capable of producing approximations of high accuracy for the mapping of such "difficult" doubly-connected domains. The essential requirement for this is that the basis set $\{u_j\}$ contains singular functions that reflect the asymptotic behaviour of the function H in the neighbourhood of each "singular" corner.

1.   **Introduction.**

Let n be a finite doubly-connected domain with boundary $\partial\Omega = \partial\Omega_1 \cup \partial\Omega_2$ in the complex z-plane, where $\partial\Omega_i$; i = 1,2, are closed Jordan curves. We assume that $\partial\Omega_i$ i = 1,2, are respectively the inner and outer components of $\partial\Omega$, and that the origin 0 lies in the "hole" of Ω, i.e. $0 \in \text{Int}(\partial\Omega_1)$.

Let ζ be a fixed point in $\overline{\Omega} = \Omega \cup \partial\Omega$ and let

$$w = f(z) , \tag{1.1}$$

be the function which maps conformally Ω onto the circular annulus

$$R = \{w : r_1 < |w| < r_2\}, \tag{1.2}$$

so that $\partial\Omega_i$; i = 1, 2, correspond respectively to $|w| = r_i$; i = 1,2, and

$$f(\zeta) = \zeta .$$

$$\tag{1.3}$$

As is well known, this mapping exists uniquely and the ratio of the two radii, i.e. the number

$$M = r_2/r_1 > 1, \tag{1.4}$$

is the so-called conformal modulus of Ω. This number determines completely the conformal equivalence class of the domain Ω.

In the present paper we consider the use of two closely related numerical methods for determining approximations to f of the form

$$f_n(z) = z \ \exp \left\{ \sum_{j=1}^{n} a_j \ u_j(z) \right\} , \tag{1.5}$$

where $\{u_j.(z)\}$ is an appropriate set of basis functions. The two methods are respectively a variational method (VM), based on an extremum property of the function

$$H(z) = f'(z)/f(z) - 1/z , $$

$$\tag{1.6}$$

and an orthonormalization method (ONM), based on approximating the function H by a finite Fourier series sum. The VM is described with full theoretical details in Gaier [4], whilst the ONM emerges easily from the theory contained in [l], [4] and [10]. The two methods resemble respectively the well-known Ritz and Bergman kernel methods for the mapping of a simply-connected domain onto the unit disc. In fact, the two numerical techniques of the present paper can be regarded as generalizations, to the mapping of doubly connected domains, of the Ritz and Bergman kernel procedures studied recently in [11].

The general objectives of the present paper are as follows. To give a summary of the theoretical results on which the VM and the ONM are based, to describe the two numerical techniques and to present a number of illustrative numerical examples. However, our main purpose is to consider the use of the two methods for the mapping of domains involving sharp corners, where branch point singularities occur. For this reason, most of the numerical examples considered in this paper concern the mapping of such difficult domains.

The numerical results given in Section 5, as well as results of other numerical experiments not presented in this paper, indicate that both the VM and the ONM are capable of producing approximations of high accuracy. More precisely, our results show that high accuracy is achieved when the domain under consideration is 2n-fold symmetric, with $n \geq 2$, provided that the basis set, used for approximating the function H, contains singular functions that reflect the asymptotic behaviour of H in the neighbourhood of a corner where a singularity occurs. Such a basis can always be con-structed, in a manner similar to that used for constructing the basis for the Ritz and the Bergman kernel methods in [11], by introducing appropriat

singular functions into the set

$$\{z^{j}\}_{j=-\infty}^{\infty} \ , \ \ j \neq -1 \ . \tag{1.7}$$

2.   Preliminary Results

We let $L_2 (\Omega)$ be the Hilbert space of all square integrable functions which are analytic and possess a single-valued indefinite integral in Ω, and denote the inner product of $L_2 (\Omega)$ by (,), i.e.

$$(g_1, g_2), = \iint_{\Omega} g_1(z) \overline{g_2(z)} \ \ dxdy \ . \tag{2.1}$$

We also let

$$A (z)=\log F(z)-\log z, \tag{2.2}$$

where f is the function(1.1) mapping Ω onto the circular annulus R. Then, the function A is analytic and single-valued in Ω, and its derivative

$$H (z) = A' (z), \tag{2.3}$$

is the function(1.6). Clearly, $H(z) \neq 0$, $z \varepsilon \Omega$, unless Ω is itself a circular annulus with its centre at the origin.

In order to present the results on which the VM is based we let

$$K^{(1)} (\Omega \Omega = \{u(z):u \in L_2(\Omega \Omega \text{ and } (u, H)=1\}$$

$$K^{(0)} (\Omega \Omega = \{v(z):v \in L_2(\Omega \Omega \text{ and } (v, H)=1\} \tag{2.4}$$

and, as in Gaier [4, p 245], we consider the following variational problem.

Problem 2.1.   To minimize

$$\|u\|^2 = \iint_{\Omega} |u(z)|^2 dxdy, \tag{2.5}$$

over all $u \in K^{(1)}(\Omega)$.

The following results are proved in [4]:

R 2.1   Problem 2.1 has a unique solution u_0.

R 2.2   The function H is related to the minimal function u_0 by

$$H(z)=u_0(z)/\|u_0\|^2. \tag{2.6}$$

R 2.3   The minimal function u_o is orthogonal to every function

$v \in K^{(0)} (\Omega)$i.e.   (2.7)

$$(u_0, v) = 0, \quad \forall v \in K^{(0)} (\Omega)$$

It is of interest to note that the above results are all special cases of standard results of the theory of Hilbert spaces. This follows from the observation that $K^{(1)} (\Omega)$ and $K^{(0)}(\Omega)$ are respectively a closed convex subset and a closed convex subspace of $L_2 (\Omega)$; see e.g. [13].

In addition to R2.1 - R2.3, the following two results, which are proved in [4, p.250], are needed for the description of both the VM and the ONM.

R 2.4   For each function $\eta \in L_2(\Omega)$which is continuous on $\partial = \partial \cup \partial$

$$(\eta , H) = i \int_{\partial \Omega} \eta (z) \log |z| dz,   (2.8)$$

where H is defined by (2.2).

R 2.5   The modulus $M = r_2/r_1$ of Ω is related to the function H by

$$\log M = \left\{ \frac{1}{i} \int_{\partial \Omega} \frac{1}{z} \log |z| dz - \| H \| 2 \right\}/2\Pi .   (2.9)$$

The result R.2.4 is established early after first expressing the inner product (η, H) as

$$(\eta, H) = \frac{1}{2i} \int_{\partial \Omega} \eta(z) \overline{A(z)} dz. .$$

This is done by means of the Green's formula

$$(g_1, g_2) = \frac{1}{2i} \int_{\partial \Omega} g_1(z) \overline{g_2(z)} dz,   (2.10)$$

which is also needed for determining certain other inner products that occur in both the VM and the ONM. As is shown in Bergman [1, p.96], formula (2.10) is valid for any functions g_1 and g_2 which are analytic in Ω and continuous on $\partial \Omega$. The result R.2.5 is established, by integration by parts, after first applying (2.8) to the norm $\|H\|^2 =(H,H)$; see [4, p.p.250-51]

5.

for further details.

We point out that the assumptions concerning the continuity on $\partial\Omega$ of the functions g_1, g_2 in (2.10) and η in (2.8) can be replaced by somewhat weaker requirements. For example, it can be shown that both (2.8) and (2.10) are applicable to "singular" functions of the type considered in Section 4.

3.   The Numerical Methods

As was previously remarked the VM is due to Gaier [4, p.249]. The method emerges by seeking the solution of the finite-dimensional counterpart of Problem 2.1, and resembles closely the Ritz method for the mapping of simply-connected domains. For this reason the VM details given below are similar to those used for the description of the Ritz method in [11].

Let $\{n_j(z)\}$ be a complete set of $L_2(\Omega)$ and denote by ${}_n^{(1)}(\Omega)$ and ${}_n^{(0)}(\Omega)$ the $n\mathfrak{C}$-dimensional counterparts of ${}^{(1)}(\Omega)$ and ${}^{(0)}(\Omega)$ corresponding to the set $\{n_j(z)\}$, i.e.

$$K_n^{(1)}(\Omega) = \{\phi_n(z) : \phi_n = \sum_{j=1}^{n} c_j n_j, c_j \in \mathfrak{C} \text{ and} (\phi_n, H) = 1\},$$

and

$$K_n^{(0)}(\Omega) = \{\psi_n(z) : \psi_n = \sum_{j=1}^{n} d_j n_j, d_j \in \mathfrak{C} \text{ and} (\psi_n, H) = 0\},$$

Then, the conditions $(\phi_n, H) = 1$ and $(\psi_n, H) = 0$ imply respectively that

$$(3.1)$$

and

$$(3.2)$$

where

$$\gamma_j = (\eta_j, H) \ ; \ j = 1, 2, \ldots \tag{3.3}$$

Since the set $(n_j(z)\}$ is complete and $H(z) \not\equiv 0$, it follows that not all the inner products γ_j are zero. In fact, for the purposes of the present paper we may assume that

$$\gamma_1 = (\eta_1, H) \neq 0 ,$$

so that the set $K_n^{(1)}(\Omega)$ is non-empty for any $n \geq 1$.

The n-dimensional variational problem corresponding to Problem 2.1 can be stated as follows.

Problem 3.1   To minimize

$$|| \phi_n ||^2 = \iint_\Omega | \phi_n(z) |^2 \ dxdy ,$$
(3.4)

over all $\phi_n \in K_n^{(1)}(\Omega)$.

The following results hold:

R 3.1   Problem 3.1 has a unique solution $\hat{\phi}_n$.

R 3.2   The minimal function $\hat{\phi}_n$ is completely characterized by the property

$$(\hat{\phi}_n, \psi_n) = 0 , \ \forall \psi_n \in K_n^{(0)}(\Omega).$$
(3.5)

R 3.3   The minimal function $\hat{\phi}_n$ converges almost uniformly in Ω to u_0. That is, from (2.6),

$$\hat{\phi}_n(z) / || \hat{\phi}_n ||^2 \to H(z) ,$$
(3.6)

almost uniformly in Ω. (By almost uniform convergence we mean convergence in every compact subset of Ω.)

The results R 3.1 and R 3.2 are of course the finite dimensional counterparts of R 2.1 and R 2.3. Like R 2.1 and R 2.3, they are particular cases of standard results of the theory of Hilbert spaces. R 3.3 is a direct consequence of the fact that in $L_2(\Omega)$ convergence in the norm implies almost uniform convergence, and it is established after
first showing that

$$\lim_{n\to\infty} || \hat{\phi}_n - u_0 || = 0$$

Let

$$\hat{\phi}_n(z) = \sum_{j=1}^{n} c_j \eta_j(z), \tag{3.7}$$

be the minimal function solving Problem 3.1. Then, the coefficients

c_i satisfy (3.1) and, from R 3.2, they must be determined so that

$$(\hat{\phi}_n, \psi_n) = 0, \quad \forall \psi_n \in K_n^{(0)}(\Omega). \tag{3.8}$$

Because of (3.2), it can be shown easily that any function

$$\psi_n(z) = \left\{ \sum_{j=1}^{n} d_j \eta_j(z) \right\} \in K_n^{(0)}(\Omega),$$

can be written in the form

$$\psi_n(z) = \frac{1}{\gamma_1} \sum_{j=2}^{n} d_j \{\gamma_1 \eta_j(z) - \gamma_j \eta_1(z)\}, \tag{3.9}$$

This implies that a necessary and sufficient condition for (3.8) to hold

is that

$$(\hat{\phi}_n, \ \gamma_1 \eta_i = \gamma_i \eta_1) = 0; i = 2,3,....,n$$

or

$$\sum_{j=1}^{n} \{\bar{\gamma}_i(\eta_j, \eta_1) - \bar{\gamma}_i(\eta_j, \eta_1)\} c_j = 0 \ ; \ i = 2,3,...,n, \tag{3.10}$$

where the inner products γ_i ; i = 1,2,...,n, are known by means of (2.8).

The n-1 equations (3.10) together with the equation (3.1) constitute

an n x n linear system for the determination of the n coefficients c_i.

That is, the coefficients c_i in (3.7) are determined by solving the linear

System

$$\left. \begin{array}{l} \displaystyle\sum_{j=1}^{n} \gamma_j c_j = 1 \\[4mm] \displaystyle\sum_{j=1}^{n} \{\bar{\gamma}_1(\eta_i, \eta_i) - \bar{\gamma}_i(\eta_j, \eta_1)\} c_j = 0; i = 2,3,.,,,.n. \end{array} \right\} \tag{3.11}$$

Then, because R 3. 3,

$$H_n(z) = \hat{\phi}_n(z) / \left\| \hat{\phi}_n \right\|^2, \tag{3.12}$$

gives the nth VM approximation to the function $H(z) = A(z)$ and thus, from (2.2),

$$f_n(z) = z \exp \left\{ \int_\zeta^z H_n(t)dt \right\} \qquad \zeta \in \overline{\Omega}, \tag{3.13}$$

is the nth VM approximation to the mapping function f.   Also, from (2.9),

$$M_n = \exp \left\{ \left(\frac{1}{i} \int_{\partial\Omega} \frac{1}{z} \log|z|dz - \|H_n\|^2 \right) / 2\pi \right\}.$$

is the nth VM approximation to the modulus M of Ω.   In fact, it can be easily verified that M_n gives an upper bound to II.

In the ONM the approximation to the mapping function f is determined after first approximating the function H by a finite Fourier series sum. The method emerges easily from the theory contained in [10, p.373], [1, p.102] and [4, p.249].

Let $\{n_j^*(z)\}$ be a complete orthonormal set of $L_2(\Omega)$. Then the function H has the Fourier series expansion

$$H(z) = \sum_{j=1}^{\infty} B_j \eta_j^*(z), \tag{3.15}$$

Where the Fourier coefficients

$$B_j = (H, n_j^*)$$
$$= \overline{(n_j^*, H)}, \tag{3.16}$$

are known by means of (2.8). The series (3.15) certainly converges in the norm of $L_2(\Omega)$ and, as in the case of R 3.3, this norm convergence implies almost uniform convergence in Ω.

Given a complete set $\{n_j.(z)\}$ of $L_2,(\Omega)$, the results (3.15) and (3.16) suggest the following procedure for obtaining a numerical approximation to the mapping function f.   The set $\{n_j(z)\}_{j=1}^n$, is orthonormalized by means of the Gram-Schmidt process to give the orthonormal set $\{n_j^*(z)\}_{j=1}^n$.

The series (3.15) is then truncated after n terms to give the approximation

$$H_n (z) = \sum_{j=1}^{n} \beta_j \, n_j^*(z),$$
$$\beta_j = \overline{(n_n^*, H)} : j = 1, 2, ..., n,$$
(3.17)

to the function H.. Finally, with this H_n, the equations (3.13) and (3.14) give respectively the nth ONM approximation to the mapping function f and to the modulus M of Ω.

The ONM can also be deduced by considering the Bergman kernel function of Ω. This is the unique reproducing kernel K (z;t),t∈Ω, of $L_2(\Omega)$, i.e. K satisfies the property

$$g(t) = (g, K), \quad g \in L_2(\Omega).$$
(3.18)

Because of the property (3.18), K has the Fourier series expansion

$$K(z; t) = \sum_{j=1}^{\infty} \overline{n_n^*(t)} \, n_j^*(z),$$
(3.19)

which, for the reasons explained above, converges almost uniformly in Ω. The connection between K and the ONM emerges by applying formula (2.8) to the inner product (K,H).   Because of (3.18), this gives

$$\overline{H(t)} = i \int_{\partial\Omega} K(z, t) \log|z| dz$$

or

$$H(t) = \frac{1}{i} \int_{\partial\Omega} \overline{K(z, t)} \log|z| \overline{dz}$$

$$= \frac{1}{i} \sum_{j=1}^{\infty} \left\{ n_j^*(t) \left(\int_{\partial\Omega} \overline{n_j^*(z)} \log|z| dz \right) \right\}$$

$$= \sum_{j=1}^{\infty} \overline{(n_j^*, H)} n_j^*(t) \quad , \quad t \in \Omega \ ,$$

which is the Fourier series (3.15) – (3.16) of H.   The above can also be

deduced easily from the results of Bergman [l,p.l02].

We end this section by observing that Problem 2.1, with the function
H defined by (2.3), is a special case of a more general variational problem which is considered fully in Gaier [4, Chap. V]. More specifically the results R 2.1 - R 2.3, together with the corresponding finite-dimensional results of this section, hold for any finitely-connected domain and any function $H \in L_2 (\Omega)$ such that $H(z) \neq 0$, $z \in \Omega$. An interesting example of this is the case where Ω is simply-connected and H is taken to be the Bergman kernel function of Ω. In this case, the results R 2.1 - R 2.3 constitute the so-called property of minimum area, and the variational method of the present section reduces to the Ritz method for the mapping of simply-connected domains. Other choices of H lead to other interesting results concerning the mapping of multiply-connected domains; see Gaier [4; Chap. V] for further details.

4.   Choice of Basis

A serious drawback of both the VM and the ONM is that severe loss of accuracy may occur during the computation, due to ill-conditioning of the matrix in (3.11) or to numerical instability of the Gram-Schmidt process. For this reason, the success of the methods depends strongly on the rate of convergence of the approximating series, and this in turn depends on the choice of basis functions $\{n_i z)\}$.

An obvious choice of basis is the set
$$\left\{z^j\right\}_{j=-\infty}^{\infty} \quad , \quad j \neq -1.$$
(4.1)
This set is complete in $L_2 (\Omega)$ and provides a computationally convenient basis for both the VM and the ONM. Unfortunately, the situation regarding

the use of (4.1) is exactly the same as that observed in [9], [11] and [12], in connection with the use of the set $\{z^j\}_{j=0}^\infty$ for the mapping of simply-connected domains by means of the Ritz and the Bergman kernel methods. That is, due to the presence of singularities of the function H in the complement of Ω, the convergence of the resulting approximating series is often extremely slow. Because of this, the use of (4.1) does not always lead to approximations of acceptable accuracy. In order to overcome this difficulty, we adopt the procedure first proposed in [9], in connection with the choice of basis for the Bergman kernel method. This involves the use of an "augmented basis", formed by introducing into the set (4.1) singular functions that reflect the main singular behaviour of H in compl (Ω).

In [9], [11] and [12], the augmented basis for the mapping of simply-connected domains is formed by considering two types of singularities of the mapping function. These are either poles which lie close to the boundary or branch point singularities on the boundary itself. For the problems considered in [9], [11] and [12], the dominant poles of the mapping function can be determined, by using the symmetry principle, whenever the boundary of the simply-connected domain consists of straight line segments and circular arcs. Unfortunately, in the case of doubly-connected domains we do not know of a systematic way for determining the poles of f and the corresponding singularities of the function H, irrespective of the geometry of $\partial\Omega$. For this reason, in the present paper we construct the augmented basis by considering only the branch point singularities of H.

Branch point singularities are corner singularities. They occur, when due to the presence of a corner at a point $z_j. \in \partial\Omega$, the asymptotic expansion of the mapping function f in the neighbourhood of $z_j.$ involves

fractional powers of $(z - z_j)$. The question regarding the choice of suitable basis functions for dealing with such singularities can be answered in exactly the same way as in [9], [11] and [12], by using the results of Lehman [8]. For this reason, we state below the formulae which define the singular functions, without repeating the details of their derivation.

Let part of the boundary $\partial\Omega$ consist of two analytic arcs Γ_1 and Γ_2 which meet at a point z_j and form there a corner of interior angle an, where a = p/q > 0 is a fraction reduced to its lowest terms. (By interior angle we mean interior to the domain Ω.) Then, the asymptotic expansion of H involves terms which can be written in the form

$$\eta_{rj}(z) = \begin{cases} \{(1/z - 1/z_j)^{r-1}\}/z^2, & \text{if } s_j \in \partial\Omega_j, \qquad (4.2) \\ (z - z_j)^{r-1}, & \text{if } z_j \in \partial\Omega_2, \qquad (4.3) \end{cases}$$

Where

$$r = k + \ell/a \; ; \; k = 0,1,2,..., 1 \le \ell \le p. \qquad (4.4)$$

Thus, if $p \ne 1$ a branch point singularity occurs at z_j. For this reason, the augmented basis is formed by introducing into the set (4.1) the first few singular functions of the sequences (4.2) or (4.3), corresponding to the first few fractional values of r.

We note that the singular functions defined by (4.3) are the same as those used in [9] and [11], for dealing with the branch point singularities of the interior mapping function for simply-connected domains. Similarly, the singular functions (4.2) are the same as those used in [12], in connection with the exterior mapping problem for simply-connected domains. This choice of singular functions ensures that the η_{rj} always have a single valued integral in Ω. We also note that a branch point singularity might occur at the point z_j even when p = 1. This happens because the asymptotic

expansion of f might involve logarithmic terms; see [8] and [11, Sect. 4.2]. However, such logarithmic singularities are never very serious and, for this reason, we do not consider them in the present paper. Finally, we note that if $z_j \in \partial\Omega$ and the arms Γ_1, Γ_2 of the corner are straight lines then the range (4.4) for the values of r in (4.3) may be replaced by

$$r = \ell/a \; ; \; \ell = 1,2,3,..... \; ; \tag{4.5}$$

see [9, Sect. 2.2] and [11, Sect. 4.2].

5.   Computational Details and Numerical Examples.

Both the VM and ONM require the evaluation of inner products of the form (η_r,η_s) and (η,H).   These are needed for determining the coefficients of the linear system (3.11), for orthonormalizing the set $\{n_j(z)\}$ by means of the Gram-Schmidt process, and for evaluating the Fourier coefficients in (3.17).   Using Green's formula (2.10), the inner products (η_r,η_s) are expressed as

$$(\eta_r,\eta_s) = \frac{1}{2i} \int_{\partial\Omega} \eta_r(z)\overline{\mu_s(z)}, \qquad \mu_s(z) = \eta_s(z), \tag{5.1}$$

and the integrals in (5.1) are then computed by Gaussian quadrature, in exactly the same way as in [9], [11] and [12]. Similarly, each inner product (η,H) is computed by applying to the integral in (2.8) the Gaussian rule used for the evaluation of (5.1).   When performing the quadrature care must be taken to deal with integrand singularities that occur when, due to the presence of a corner at z_j, the basis set contains singular functions of the form (4.2) or (4.3). In the examples considered below, the arms of the corners are always straight line segments, and any intergrand singularities are removed, as explained in [9, Sect. 3], by choosing an appropriate parametric representation for $\partial\Omega$; see also [11, Sect. 5] and [12, Sect. 3].

In the VM, the complex linear system (3.11) is solved by using the NAG Library routine F04ADF, which is based on Crout's factorization method.

In the ONM, the orthonormalization is performed by means of the procedure used in [9], [11] and [12], in connection with the Bergman kernel method. This procedure is based on the standard Gram-Schmidt algorithm.

The approximation M_n to the modulus M of Ω is computed from (3.14), by applying to the integral

$$\frac{1}{i}\int_{\partial\Omega}\frac{1}{z}\log|z|dz,$$

the Gaussian rule used for the evaluation of the inner products (η_r,η_s) and (η,H).

An estimate of the maximum error in $|f_n(z)|$ is given by the quantity E_n, which is determined as follows. In each example, the fixed point ζ in (1.3) is taken to be a convenient point on the outer boundary $\partial\Omega_2$. Thus, in each case, the outer radius of the annulus is

$$r_2 = |\zeta|, \tag{5.2}$$

and r_2/M_n gives an approximation to the inner radius r_1 . Hence, we may take the error estimate to be

$$E_n = \max\{{}^{\max}_j\left|\left|f_n(z_{1j})\right|-r_2/M_n\right| \;,\; {}^{\max}_j\left|\left|f_n(z_{2j})\right|-r_2\right|\}, \tag{5 3}$$

where $\{z_{1j}\}$ and $\{z_{2j}\}$ are two sets of "boundary test points" on $\partial\Omega_1$ and $\partial\Omega_2$ respectively. We expect E_n to be a reasonable error estimate, because our numerical experiments indicate strongly that, in general, the approximation M_n is much more accurate than $|f_n(z)|$, $z\in\partial\Omega$; see e.g. the numerical results of Example 5.2.

In each example, the ONM results presented correspond to the approximation f_{Nopt}, where n = Nopt is the "optimum number" of basis functions which gives maximum accuracy in the sense explained in [9, Sect. 3]. That is, this number is determined by computing a sequence of approximations

$\{f_n(z)\}$, where at each stage the number n of basis functions is increased
by one. If at the (n+l)th stage the inequality

$$E_{n-1} < E_n, \qquad\qquad\qquad (5.4)$$

is satisfied then the approximation $f_{+o}(z)$ is computed. When for a
certain value of n, due to numerical instability, (5.4) no longer holds
then we terminate the process and take n = Nopt. Also, in order to
safeguard against slow convergence, we do as in [12] and after n = 19
we begin to compute the ratios

$$q_M = E_{IO+M}; \quad M = 10,20,....$$

If, for some M, $q_M > 0.5$ than we terminate the process at n = 10 + M

and write $N_{opt}^* = 10 + M.$

For the presentation of the results we adopt a format similar to
that used in [11]. That is, we denote the two methods respectively
by VM/MB and 0NM/MB or VM/AB and 0NM/AB to indicate whether the "monomial
basis" (4.1) or an "augmented basis" is used. For each example we
list the singular functions, the boundary test points and the order of
the Gaussian quadrature, which are used respectively for augmenting the
set (4.1), for determining the error estimate (5.3) and for computing
the inner products. As was previously remarked, if the basis set
contains singular functions of the form (4.2) or (4.3) then the resulting
integrand singularities in the inner products are removed by using special
parametric representations for $\partial\Omega$. These representations are similar to
those used in [9, Sect. 3].   For this reason, we do not list them here.

All computations were carried out on a CDC 7600 computer, using programs
written in Fortran with single precision working. Single length working
on the CDC 7600 is between 13 and 14 significant figures.

Example 5.1. Circle in square; Figure 5.1.

$$\Omega = \{(x,y): |x|<1, \ |y|<1\} \cap \{z: |z|>a, \ a<1\}.$$
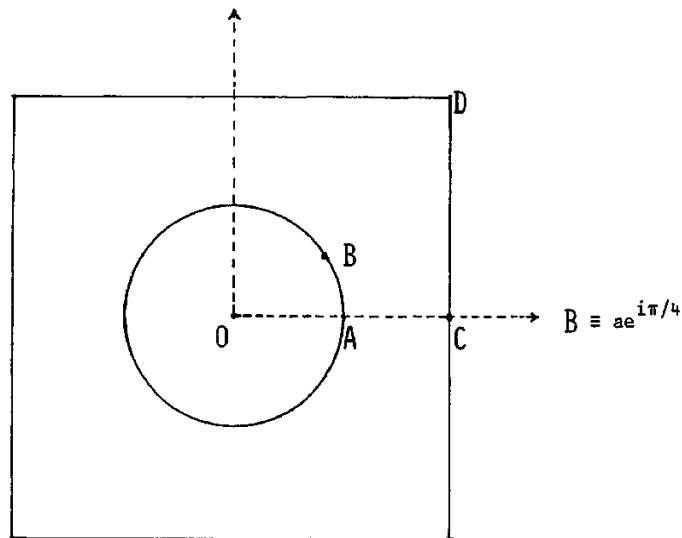

FIGURE 5.1

Basis. This example does not involve corner singularities. For this reason, we do not need to use an augmented basis.

Because the domain has eightfold symmetry about the origin the monomial basis set is taken to be

$$z^{k_j(2j+1)}, k_j = (-1)^{j+1}; j = 1,2,3,..... \tag{5.5}$$

Quadrature. Gauss-Legendre formula with 48 points along each quarter of the circle and each half side of the square.

Boundary Test Points. Because of the symmetry, we only consider points
on AB and CD. On AB the points are defined by $z = ae^{i\tau} \ \tau = 0(\pi/16)\pi/4$.

On CD the points are equally spaced, in steps of 0.25, starting from C.

<u>Numerical Results</u>.

(i)   a=0.2

ONM/MB : Nopt = 20, $E_{20} = 9.5x10^{-12}$, $M_{20} = 5.393\ 525\ 710\ 616$.

VN/MB : $E_{20} = 9.0x10^{-12}$,   *

(ii)   a = 0.4

ONM/MB : Nopt = 22, $E_{22} = 5.2x10^{-12}$, $M_{22} = 2.696\ 724\ 431\ 230$.

VM/MB : $E_{22} = 3.1x10^{-12}$,   *

(iii)   a = 0.8

ONM/MB : Nopt = 28, $E_{28} = 1.8x10^{-10}$, $M_{28} = 1.342\ 990\ 365\ 599$.

VM/MB : $E_{28} = 7.0X10^{-11}$,   *

(* In each case the VM approximation to M agrees with the ONM approxi-
mation to the number of figures quoted.)

The numerical results of this example illustrate the remarkable
accuracy that can be achieved by the VM/MB and the ONM/MB, when the
domain under consideration is highly symmetric and does not involve
corner singularities.

Accurate VM/MB approximations for the cases a = 0.4 and a = 0.8
have also been obtained by Gaier. His approximations to M are quoted
to seven significant figures in [5], and agree perfectly with the
approximations listed above. The approximation M_{22}, corresponding to
the case a = 0.4, should also be compared with the value 2.696 725 given
in [11]. This value is obtained by a method based on approximating
the conformal map onto the unit disc, of the simply-connected domain
bounded by the arc AB and the straight lines BD, DC and CA; see [11,
Ex. 6.3].

Example 5.2.   Square frame;   Figure 5.2.

Let

$$G_a = \{(x,y) : |x| < a, |y| < a\}.$$

Then

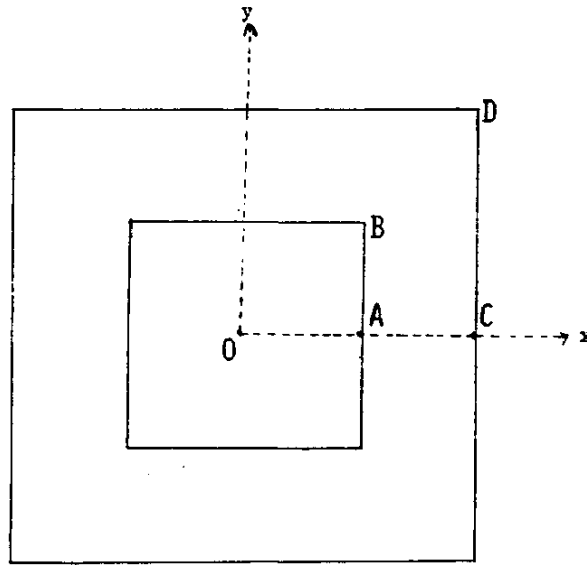$$\Omega = G_1 \cap \text{compl} \, (\overline{G}_a) \, , \text{with a} < 1.$$

FIGURE 5.2

Augmented Basis. Because the domain has eightfold symmetry about the origin, the monomial basis is taken to be the set (5.5).

Let z_j ; j = 1,2,3,4, be respectively the four corners of the inner square. Then, the singular functions corresponding to the branch point singularities at the corners z_j ; j = 1,2,3,4 are respectively the functions $n_{\gamma j}(z)$; $j = 1,2,3,4,$ given by (4.2) with

$$r = k + 2\ell/3, \quad k = 0,1,...., 1 \le \ell \, 1 \le 3. \tag{5.6}$$

Because of the eightfold symmetry the function H(z) satisfies the property

$$e^{i\pi/2}H(e^{i\pi/2}z) = H(z)$$

For this reason, for each value of r, the four functions $n_{rj}(z)$ can be combined into the single function

$$\widetilde{\eta}_r(z) = \eta_{r1}(z) + \sum_{j=2}^{4} e^{i\theta} \eta_{rj}(z) \quad , \tag{5.7}$$

where the arguments θ_j ; j= 2,3,4 are chosen so that

$$e^{i\Pi/2} \eta_r(e^{i\Pi/2}z) = \eta_r(z). \tag{5.8}$$

It is important to observe that the constants θ_j in (5-7) depend on the branches used for defining the functions $\eta_{rj}(z)$. For this reason, great care must be taken when constructing symmetric singular functions of the form (5.7).

In this example the augmented basis is formed by introducing into the set (5.5) the four singular functions (5.7) corresponding to the values r = 2/3, 4/3, 5/3, 7/3.

Quadrature. Gauss-Legendre formula with 48 points along each side of the outer square and each half side of the inner square. In order to perform the intergration accurately, the parametric representation of the inner square is chosen to be that used in [12, Ex.3.2].

Boundary Test Points. Because of the symmetry, we only consider points on AB and CD. The points are equally spaced, in steps of 0.25, starting from A and C respectively.

Numerical Results.

<div align="center">(i) a = 0.2</div>

ONM/MB : N^*_{opt} = 30, E_{30} = 1.8×10^{-2} , M_{30} = 4.575 2.........

ONM/AB : Nopt = 24, E_{24} = 1.1×10^{-8} , M_{24} = 4.570 859 677 117.

VM/AB   : E_{24} = 1.1×10^{-8} , M_{24} = 4.570 859 677 116.

<div align="center">Exact value of M = 4.570 859 677 215.</div>

<div align="center">(ii) a = 0.5</div>

ONM/MB : N^*_{opt} = 30, E_{30} = 4.3×10^{-2} , M_{30} =   1.856 9.................

ONM/AB : Nopt = 24, E_{24} = 5.0×10^{-8} , M_{24} =   1.847 709 011 217.

VM/AB   : E_{24} = 5.0×10^{-8} , M_{24} =   1.847 709 011 216.

<div align="center">Exact value of M = 1.847 709 011 236.</div>

<div align="center">iii) a = 0.8</div>

ONM/MB : N^*_{opt} = 30, E_{30} = 5.0×10^{-2} , M_{30} = 1.205 2 ....

ONM/AB : Nopt = 26, E_{26} = 3.7×10^{-7} , M_{26} = 1.201 452 809 479.

VM/AB   : E_{26} = 4.1×10^{-7} , M_{26} = 1.201 452 809 478.

<div align="center">Exact value of M = 1.201 452 809 469.</div>

The exact values of M, listed above, were computed by using the exact formulae of Bowman [2] and [3, p.104].

VM approximations to M have also been computed by Gaier and his students [6], who used as basis the set (5.5) augmented with the single singular function

$$1/\{z^{11/3}(z^4 + 4a^4)^{1/3}\}.$$

For the case a = 0.5, their approximation to M is 1.847 776. For the same case, by using an approximation to the conformal map of the quadric-lateral ABDC the method of [11] gives the value 1.847 719; see [11, Ex.6.1],

Example 5.3.   Rectangle in circle; Figure 5.3.

Let

$$G_{ab} = \{(x,y) : |x| < a < 1, \qquad |y| < b < 1\} \ .$$

Then

$$\Omega = \{z : |z| < 1\} \ \bigcap \ \text{compl}(\overline{G}_{ab}).$$
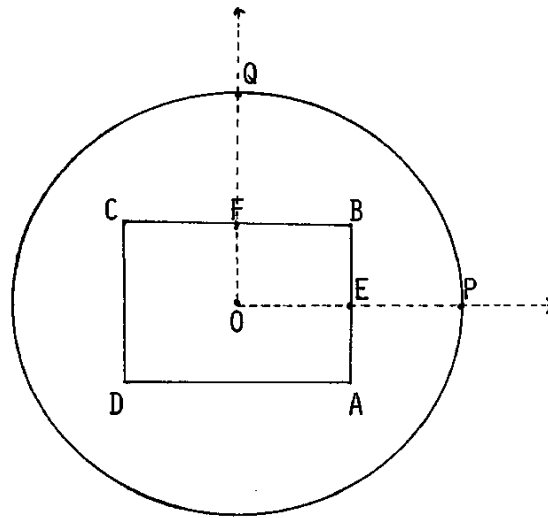

FIGURE 5.3

Augmented Basis.   When $a = b$, Ω has eightfold symmetry about the origin and, for this reason, the monomial basis is taken to be the set (5.5).

When $a \neq b$, Ω has fourfold symmetry about O. Because of this, the function H satisfies

$$e^{i\pi}H(e^{i\pi}z) = H(z),$$

and the monomial basis is taken to be the set

$$z \ , \ z^{\pm(2j+1)} \ ; \quad j = 1,2,3,\ldots.$$

(5.9)

Let z_j ; j = 1,2,3,4, be respectively the corners A, B, C and D of the rectangle. Then, the singular functions corresponding to the

branch point singularities at z, ; j = 1,2,3,4, are respectively the functions $\eta_{rj}(z)$; j = 1,2,3,4 defined by (4.2) with r given by (5.6).

When a = b then, for each value of r, the four functions $\eta_{rj}(z)$ can be combined into a single function of the form (5.7) - (5.8). Similarly, because of the fourfold simmetry, when a ≠ b, for each value of r, the four functions $\eta_{rj}(z)$ can be combined into the two functions

$$\widetilde{\eta}_{rj}(z) = \eta_{rj}(z) + e^{i\theta}\eta_{r,j+2}(z) \; ; \quad j = 1,2, \qquad (5.10)$$

where the arguments θ_j ; j = 1,2, are chosen so that

$$e^{i\Pi}\widetilde{\eta}_{rj}(e^{i\Pi}z) = \widetilde{\eta}_{rj}(z) . \qquad (5.11)$$

In this example we form the augmented basis, for the cases a = b and a ≠ b, by introducing respectively into the monomial sets (5.5) and (5.9) the four functions (5.7) and the eight functions (5.10) corresponding to the values r = 2/3, 4/3, 5/3, 7/3.

Quadrature. Gauss-Legendre formula with 48 points along each half side of the rectangle and each quarter of the circle. In order to perform the integration accurately the parametric representation of the rectangular boundary is chosen to be that used in [12, Ex.3.2].

Boundary Test Points. Because of the symmetry we only consider points on the straight lines EB, BF and on the arc PQ. On EB and BF the points are equally spaced in steps of b/4 and a/4 respectively. On PQ the points are defined by $e^{i\tau}$; $\tau = 0(\pi/8)\pi/2$.

Numerical Results.

<div align="center">(i) a = b = 0.5</div>

0NM/MB : N_{opt}^{*} = 30, E_{30} = 5.1x10^{-2} , M_{30} = 1.702 0.........

0NM/AB : N_{opt} = 24, E_{24} = 7.0x10^{-8} , M_{24} = 1.691 564 902 59

VM/AB   : E_{24} = 7.0x10^{-8} ,   *

<u>(ii)   a = 0.4, b = 0.2</u>

ONM/AB : Nopt = 18, $E_{18} = 5.0 \times 10^{-6}$, $M_{18} = 2.849\ 771\ 072$.

VM/AB : $E_{18} = 5.0 \times 10^{-6}$,   *

<u>(iii) a = 0.6, b = 0.2</u>

ONM/AB : Nopt = 26, $E_{-26} = 1.4\ 10^{-5}$, $M_{26} = 2.133\ 835\ 1$.

VM/AB   : $E_{26}\ = 1.2\ 10^{-5}$,   *

<u>(iv) a = 0.8, b = 0.2</u>

ONM/AB : Nopt = 22, $E_{22} = 2.3\ 10^{-4}$, $M_{22} = 1.626\ 912\ 4$.

VM/AB   : $E_{22} = 2.3\ 10^{-4}$,   *

(* In each case the VM/AB approximation to M agrees with the ONM/AB approximation to the number of figures quoted.)

<u>Example 5.4.</u>   Triangle in triangle; Figure 5.4.

Let G_h denote an equilateral triangle of height h, orientated so that its centroid is at the origin and one of its sides is parallel to the real axis.
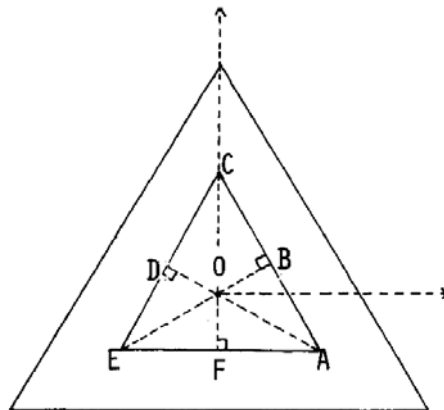

<u>FIGURE 5.4</u>

Then,

$$\Omega = G_3 \cap compl\ (G_h),\ with\ h < 3.$$

<u>Augmented Basis</u>. Because the domain has sixfold symmetry about the origin, the monomial basis is taken to be the set

$$Z^{(3j-1)}\ ;\ j = \pm 1,\ \pm2,\ \pm3,\ \dots\ . \tag{5.12}$$

Let z_j ; $j = 1,2,3$ be respectively the corners A,C,E of the inner triangle. Then, the singular functions corresponding to the branch point singularities at z_j ; $j = 1,2,3$ are respectively the functions $\eta_{rj}(z)$; $j = 1,2,3$, given by (4.2) with

$$r = k + 3\ell/5\ ;\quad k = 0,1,2,\dots\ ,\quad 1 < \ell < 5\ .$$

Because of the symmetry, for each value of r, the three functions $\eta_{ri}(z)$ can be combined into the single function

$$\widetilde{\eta}_r(z) = \eta_{r1}(z)\ +\ \sum_{j=2}^{3} e^{i\theta_j}\eta_{rj}(z)\ , \tag{5.13}$$

where the arguments θ_j ; $j = 2,3$, are chosen so that

$$e^{2\pi i/3}\eta_r(e^{2\pi i/3}z) = \widetilde{\eta}_r(z). \tag{5.14}$$

In this example the augmented basis is formed by introducing into the set (5.12) the four functions (5.13) corresponding to the values $r = 3/5,\ 6/5,\ 8/5,\ 9/5$.

<u>Quadrature</u>. Gauss-Legendre formula with 48 points along each half side of the inner and outer triangles. In order to perform the quadrature accurately the parametric representation of the inner triangle is chosen to be that used in [12, Ex. 3.3].

<u>Boundary Test Points</u>. Eighteen points distributed along the half sides BC, CD of the inner triangle and the corresponding half sides of the

outer triangle.

<u>Numerical Results</u>.

<u>(i)   h = 2.25</u>

ONM/MB : Nopt^{*} = 30, E_{30} = 1.3 10^{-1} , M_{30} = 1.227 0.......

ONM/AB : Nopt = 18, E_{18} = 7.8 10^{-5} , M_{18} = 1.208 168 761 .

VM/AB   : E_{18} = 7.8 10^{-5} ,   *

<u>(ii) h = 1.50</u>

ONM/AB : Nopt = 22, E_{22} = 6.8 10^{-7} , M_{22} = 1.657 038 875 .

VM/AB   : E_{22} = 6.8 10^{-7} ,   *

<u>(iii) h = 0.75</u>

ONM/AB : Nopt = 16, E_{16} = 7.0 10^{-6} , M_{16} = 3.132 784 643 .

VM/AB   : E_{16} = 7.0 10^{-6} ,   *

(* In each case the VM/AB approximation to M agrees with the ONM/AB approximation to the number of figures quoted.)

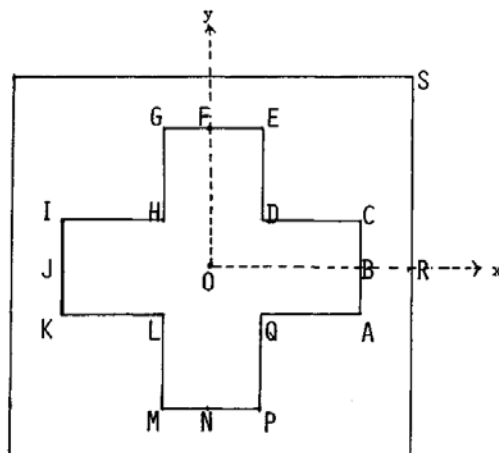<u>Example 5.5.</u>   Cross in square; Figure 5.5.

<u>FIGURE 5.5</u>

Let

$$G_{ab} = \{ (x,y) : |x| < a, |y| < b \} \cup \{ (x,y) : |x| < b, |y| < a \}, \qquad (5.15)$$

and

$$G_c = \{ (x,y) : |x| < c, |y| < c \} \ .$$

Then

$$\Omega = G_c \cap \mathrm{compl} \ (\overline{G}_{ab}) \ \text{with} \ a < c \ \text{and} \ b < c.$$

<u>Augmented Basis</u>. Because the domain has eightfold symmetry about the origin, the monomial set is taken to be the set (5.5).

Let z_j ; j = 1,2,...,8 be respectively the corners A, C, E, G, I, K, M and P of the cross shaped region G_{ab}. Then the singular functions corresponding to the branch point singularities at z_j ; j = 1,2,...,8 are respectively the functions $\eta_{rj}(z)$; j = 1,2,...,8, defined by (4.2) with r given by (5.6). Because of the symmetry, for each value of r, the eight singular functions $\eta_{rj}(z)$ can be combined into the two functions

$$\widetilde{\eta}_{rj}(z) \ = \ \eta_{rj}(z) \ + \ \sum_{m=1}^{3} e^{i\theta_{2m+j}} \ \eta_{r,2m+j}(z) \ ; \ j=1,2, \qquad (5.16)$$

where, as in (5.7), the arguments θ_{2m+j} are chosen so that

$$e^{i\pi/2}\widetilde{\eta}_{rj}(e^{i\pi/2}z) = \widetilde{\eta}_{rj}(z) \ ; \qquad j=1,2.$$

In this example the augmented basis is formed by introducing into the set (5.5) the six singular functions (5.16) corresponding to the values   r = 2/3, 4/3, 5/3.

<u>Quadrature</u>. Gauss Legendre formula with 48 points along each of the segments AB, BC, CD,..., QA, of the inner boundary, and each side of the square. In order to perform the quadrature accurately the parametric representation of the innder boundary is chosen to be that used in [12, Ex.3.5].

<u>Boundary Test Points</u>. Seventeen points on the inner boundary segment BCDEF and seventeen points on the side RS of the square.

<u>Numerical Results</u>. The upper and lower bounds for the modulus M, listed below, are due to Jauer [7], and were obtained by using a finite-element method. The comparison values $\widetilde{M}$ were computed, as in [11, Ex. 6.4], by using an approximation to the conformal map of the pentagonal domain bounded by the straight lines BR, RS, SD, DC and CB.

<u>(i) a = 0.5, b = 1.2, c = 1.5</u>

ONM/MB : Nopt = 14, $E_{14} = 9.5 \times 10^{-2}$, $M_{14} = 1.349\ 0$ ....

ONM/AB : Nopt = 21, $E_{21} = 3.8 \times 10^{-5}$, $M_{21} = 1.331\ 473\ 449$.

VM/AB   : $E_{21} = 3.8 \times 10^{-5}$,   *

<u>Comparison value</u> : $\widetilde{M} = 1.331\ 463$.

<u>Bound</u> : $1.331\ 003 < M < 1.331\ 944$.

<u>(ii) a = 0.5, b = 1.0, c = 1.5</u>

ONM/AB : Nopt = 27, $E_{27} = 8.3 \times 10^{-6}$, $M_{27} = 1.566\ 289\ 179$.

VM/AB   : $E_{27} = 8.3 \times 10^{-6}$,   *

<u>Comparison value</u> : $\widetilde{M} = 1.566\ 274$.

<u>Bound</u> : $1.565\ 602 < M < 1.566\ 978$.

<u>(iii) a = 0.2, b = 0.7, c = 1.2</u>

ONM/AB : Nopt = 25, $E_{25} = 3.0 \times 10^{-5}$, $M_{25} = 1.981\ 644\ 1$.

VM/AB   : $E_{25} = 2.8 \times 10^{-5}$,   *

<u>Comparison value</u> : $\widetilde{M} = 1.981\ 774$.

<u>Bound</u> : $1.979\ 574 < M < 1.983\ 722$.

(iv) $a = 0.1$, $b = 0.8$, $c = 1.1$

ONM/AB : Nopt = 23, $E_{23} = 3.6 \ 10^{-4}$, $M_{23} = 1.747 \ 492 \ 5$.

VM/AB   : $E_{23} = 4.0 \ 10^{-4}$,   *

Comparison value : $\widetilde{M} = 1.747 \ 677$.

Bound : $1.745 \ 050 < M < 1.749 \ 940$.

(* In each case the VM/AB approximation to M agrees with the ONM/AB approximation to the number of figures quoted.)

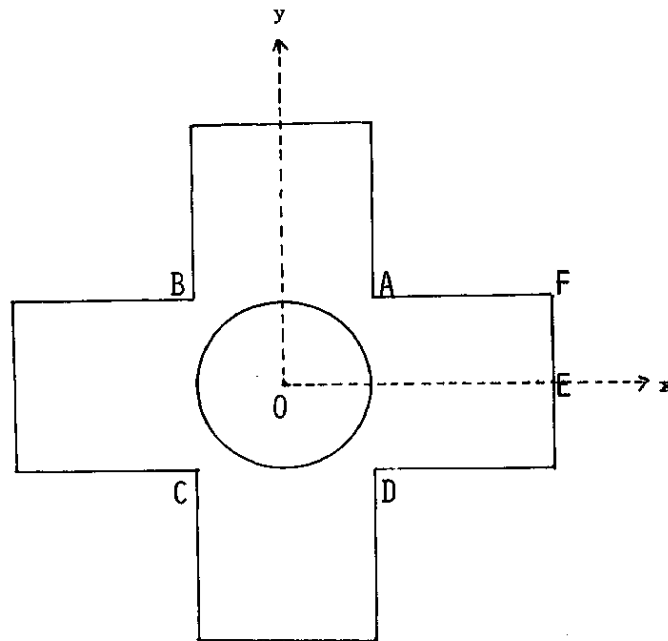Example 5.6.   Circle in cross; Figure 5.6

FIGURE 5.6

As in Example 5.5., let G_{ab} denote the cross-shaped region defined by (5.15). Then,

$$\Omega = G_{3,1} \bigcap \{z \colon |z| > c\}.$$

Augmented Basis.   Because the domain has eightfold symmetry about the origin, the monomial set is taken to be the set (5.5).

Let z_j ; j = 1,2,3,4, be respectively the corners A, B, C and D of the outer boundary. Then, the singular functions corresponding to the branch point singularities at z_j ; j = 1,2,3,4, are respectively the functions $\eta_{rj}(z)$; j = 1,2,3,4 given by (4.3) with

   r = 2l/3 ; l = 1,2,3,... .

Because of the symmetry, for each value of r, the four functions $\eta_{rj}(z)$ can be combined, as in Examples 5.2 and 5.3, into a single function $\tilde{n}_r(z)$ of the form (5.7) - (5.8). The augmented basis is formed by introducing into the set (5.5) the four functions $\tilde{n}_r(z)$ corresponding to the values r = 2/3, 4/3, 8/3, 10/3.

Quadrature.   Gauss-Legendre formula with 48 points along each side of the outer boundary and each quarter of the circle.

Boundary Test Points.   Thirteen equally spaced points on the straight lines EF and FA of the outer boundary, and six points on the circle. The test points on the circle are defined by. $ce^{i\tau}$; $\tau = 0(\pi(\pi/20)\pi$

Numerical Results.

<div align="center">(i) c = 0.8</div>

ONM/MB : $N\overset{*}{op}t$ = 30, E_{30} = 6.1x10^{-1} , M_{30} = 2.356 0.......

ONM/AB : Nopt = 22, E_{22} = 1.5x10^{-5} , M_{22} = 2.246 094 81 .

VM/AB   : E_{22} = 1.3x10^{-5} ,   *

<div align="center">(ii) c = 0.5</div>

ONM/AB : Nopt = 24, E_{24} = 7.8x10^{-6} , M_{24} = 3.595 639 19 .

VM/AB E_{24} = 8.9x10^{-6} ,   *

<div align="center">(iii) c = 0.2</div>

ONM/AB : Nopt = 24, E_{24} = 8.0x10^{-6} , M_{24} = 8.989 209 95 .

VM/AB   : E_{2k} = 8.9x10^{-6} ,   *

(* In each case the VM/AB approximation agrees with the ONM/AB approximation to the number of figures quoted.)

6. Discussion

The results of Section 5, as well as results of other numerical experiments not presented here, indicate that both the VM and the ONM are capable of computing approximations of high accuracy. In particular, our results show that the two methods can produce accurate approximations for the mapping of difficult domains, involving sharp corners. The essential requirement for this is that the basis set contains functions that reflect the asymptotic behaviour of the function H, in the neighbourhood of a corner where a singularity occurs. Regarding computational efficiency, our experiments show that the two methods require approximately the same computational effort for producing approximations of comparable accuracy.

The above remarks apply only to the mapping of domains with 2n-fold symmetry $n \geq 2$, of the type considered in Section 5. For such symmetrical domains the number of basis functions used in the numerical process can be reduced considerably and, in general, the two methods are extremely accurate. Unfortunately, in the absence of 2n-fold symmetry, $n \geq 2$, the performance of both the VM and the ONM is rather disappointing. If the domain involves "singular" corners then the use of functions of the form (4.2) or (4.3) always leads to some improvement in accuracy. However, if Ω is a non-symmetrical domain then dealing with corner singularities alone is not sufficient for the methods to produce accurate approximations. The difficulty in this case might be due to the presence of poles of the function H in $\text{compl}(\overline{\Omega})$. Unfortunately, as we remarked earlier, we do not know of a way for dealing with such singularities.

REFERENCES

[1] S. Bergman, The kernel function and conformal mapping,
     Math. Surveys 5, A.M.S., Providence, R.I., 1970.

[2] F. Bowman, Notes on two-dimensional electric field problems,
     Proc. London Math. Soc. 39 (1935), pp.205-215.

[3] F. Bowman, Introduction to elliptic functions, English
     University Press, London, 1953.

[4] D. Gaier, Konstructive Methoden der konformen Abbildung,
     Springer-Verlag, Berlin, 1964.

[5] D. Gaier,   Das logarithmische Potential und die konforme
     Abbildung mehrfach zusammenhängender Gebiete, in:
     E.B. Christoffel, The influence of his work on Mathematics
     and the Physical Sciences, Birkhäuser Verlag, Basel, 1981, pp.290-303.

[6] W. Eidel, Konforme Abbildung mehrfach zusammenhängender
     Gebiete durch Lösung von Variationsproblemen, Diplomarbeit
     Giessen, 1979.

[7] H.J. Jauer, Die Finite-Element-Methode bei Gebieten mit Krummlinigem
     Rand, Diplomarbeit Giessen, Justus-Liebig-Universität, Giessen,
     1981.

[8] R.S. Lehman, Development of the mapping function at an analytic
     corner, Pacific J. Math. 7 (1957), pp. 1437-1449.

[9] D. Levin, N. Papamichael and A. Sideridis, The Bergman kernel
     method for the numerical conformal mapping of simply-connected
     domains, J.Inst. Math. Applics. 22 (1978), pp. 171-187.

[10] Z. Nehari, Conformal Mapping, McGraw-Hill, New York, 1952.

[11] N. Papamichael and C.A. Kokkinos, Two numerical methods for the
     conformal mapping of simply-connected domains, Comput.Meths
     Appl. Mech. Engrg. 28 (1981), pp. 285-307.

[12] N. Papamichael and C.A. Kokkinos, Numerical conformal mapping of
     exterior domains. To appear in: Comput.Meths Appl. Mech.
     Engrg.

[13] J. D. Pryce, Basic Methods of Functional Analysis, Hutchinson
     University Library, London 1973.

NOT TO BE REMOVED
FROM THELIBRARY